Organometallic Stability and Structure: Elementary Rates of Unimolecular Decomposition in Chromium Olefin Carbonyls

Bruce McNamara, Marcy H. Towns, and Edward R. Grant*

Contribution from the Department of Chemistry, Purdue University, West Lafayette, Indiana 47907

Received July 21, 1995[⊗]

Abstract: Time-resolved infrared absorption has been applied to obtain elementary rates of unimolecular decomposition in the gas phase for the chromium carbonyl complexes of ethylene, propylene, 1-butene, *cis*-2-butene, *trans*-2-butene, and isobutene. Observed rates fit a trend of declining stability with increasing alkyl substitution. Arrhenius parameters, derived from the temperature dependence of the elementary unimolecular decay rate, establish that the source of this stability trend lies not in decreasing bond strengths—activation energies are essentially constant for the series—but rather in a substantial increase in the *A* factor for the larger leaving olefins. This effect is explained in terms of sterically constrained torsional and C−C−C skeletal bending vibrations that are released as the molecule dissociates, adding to the statistical driving force that favors decomposition. This suggestion is confirmed by a simplified RRKM unimolecular rate theory model that quantitatively reproduces the observed rates.

I. Introduction

The interaction of transition metals with olefins has been an important concern of organometallic chemistry for a great many years. Metal-mediated insertion and addition reactions at sites of C−C unsaturation form a major route for catalytic and stoichiometric carbon−carbon and carbon−hydrogen bond-making.[1] The efficiencies of such processes are sensitively affected by subtle changes in reaction rates and branching ratios. Steric effects in particular have long been exploited to achieve regio- and stereoselectivity in a large number of organometallic transformations.[2] Steric factors are well known to significantly alter the stability and reactivity of transition-metal olefin complexes. For reactions in solution, detailed understanding of such effects must include solvation and the role it plays in regulating the free energies of reactants and transition structures. Theory has progressed in describing intramolecular factors affecting substituted olefin bond energies,[3] but such calculations most often pertain to the gas phase, where systematic experimental results have not been available.

Experiments probing stability in the gas phase clearly provide the most fundamental view of factors that determine reactivity and selectivity in a ligand family. Such experiments present some special challenges, however. Organotransition metal intermediates easily cluster in the gas phase, and the extraction of energetics information from kinetics experiments demands great accuracy in sample preparation and rate measurement. Thus, systematic determination of such parameters as elementary rates and activation energies for metal−olefin decomposition has not been achieved for a complete ligand family, despite the importance of such information for resolving questions of bonding and the source of stability trends as a function of substituents.

We have recently made substantial progress in developing experimental methods for extracting accurate Arrhenius parameters for gas phase metal−ligand decomposition reactions.[4] In the present work, we have applied these methods to study the kinetic factors at work in determining stability for a protypical series of carbonylchromium−olefin complexes, with the olefin ranging from ethylene to isobutylene. We quantify trends in terms of the energetic and entropic factors that drive elementary unimolecular decomposition in the gas phase. The results are surprising. Gas phase stabilities follow an order that mirrors the stability of similar compounds studied in solution; more substitued olefins bond less securely. However, we find that the fundamental kinetic basis for decay rate enhancement in more hindered systems lies not in the bond strength (activation energy), but rather in the preexponential. We explain this result in terms of statistical aspects of unimolecular decay in the presence of steric constraints. The factors we identify as regulating metal-complex stability have broader implications for issues of molecular recognition in general. We quantify the behavior observed for the transition-metal olefin systems using an elementary RRKM unimolecular rate theory model.

II. Experimental Section

Ethylene, propylene, 1-butene, *cis*- and *trans*-2-butene, and isobutene, purchased from Aldrich, are used without further purification. UHP carbon monoxide (99.999%), obtained from Matheson or Airco, is passed through a liquid N_2 trap to remove what appears to be a $Fe(CO)_5$ contaminant. The contaminant absorbs in the infrared with features at 2013.44 and 2033.69 cm^{-1} and probably results from CO scrubbing of the container wall. $Cr(CO)_6$ from Alpha Products is frequently sublimed and undergoes a feeze-pump-thaw cycle before each sample filling. The stainless steel cell has a cross configuration and is fitted with 2 mm thick quartz and CaF_2 flats. The arms of the cell can be fitted with a glass liner, which has 1.27 cm ports to allow passage of the IR probe.[5]

We acquire absorbance versus time data using a Mattson Galaxy 6021 Fourier transform infrared spectrometer. For shorter time decays, we monitor transient absorption at selected frequencies using an infrared glower in combination with a J-Y 0.25 M monochromator and an InSb detector. Our general methodology and details of both instruments

[⊗] Abstract published in *Advance ACS Abstracts*, December 1, 1995.

(1) (a) Darensbourg D. J. *Adv. Organomet. Chem.* **1982**, *21*, 113. (b) Crabtree, R. H. *The Organometallic Chemistry of the Transition Metals*; Wiley-Interscience: New York, 1994.

(2) Jordan, R. B. *Reaction Mechanism of Inorganic and Organometallic Systems*; Oxford University Press: New York, 1991.

(3) (a) White, D.; Brown, T. L. To be published. (b) Brown, T. L.; Lee, K. J. *Coord. Chem. Rev.* **1993**, *128*, 89.

(4) (a) McNamara, B.; Becher, D. M.; Towns, M. H.; Grant, E. R. *J. Phys. Chem.* **1994**, *98*, 4622. (b) Weiller, B. H.; Grant, E. R. *J. Phys. Chem.* **1988**, *92*, 1458.

(5) Rate measurements were reproduced at room temperature in a Pyrex cell and over many compositions and temperatures in the stainless steel cell outfitted with a Pyrex liner.

0002-7863/95/1517-12254$09.00/0 © 1995 American Chemical Society

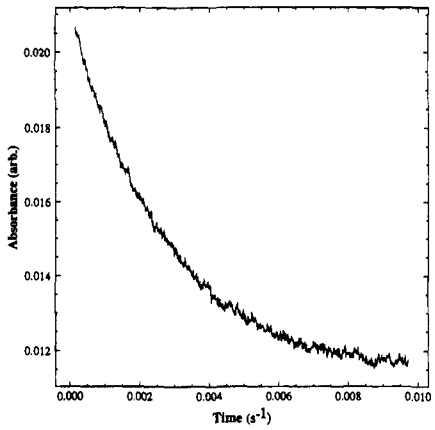

Figure 1. Absorbance decay at 80 °C for $Cr(CO)_5(cis\text{-}2\text{-}C_4H_8)$. Absorbance decay is generally followed for 5 half-lives to establish a reliable baseline. Fits for k_{obs} use an adjustable offset parameter.

have been reported elsewhere.[4,6] A Lambda Physik EMG 101 excimer laser supplies 15 ns pulses of 308 nm light for photolysis. In the FTIR experiment, we use laser powers between 20 and 100 mJ/pulse and repetition rates below 5 Hz. Higher average powers deposit $Cr(CO)_6$ fragmentation products on the UV entrance window. Higher CO concentrations and temperatures used in the TRIR experiment allow for laser powers in excess of 300 mJ/pulse.

Irradiation of gaseous mixtures of olefin, CO, and $Cr(CO)_6$ produces the $Cr(CO)_5$(olefin) complex. The range of concentration in these experiments varies from $0.01 < [olefin]/[CO] < 500.0$. This corresponds to a change in k_{obs} which spans 8 orders of magnitude. The k_{obs} data are obtained from three-parameter nonlinear fits to well-behaved, single-exponential absorbance versus time curves, as shown in Figure 1. In both the FTIR and TRIR experiments, reactions are normally followed for over 5 half-lives. Rate data are acquired between 20 and 100 °C. The temperature of the cell interior is monitored to an accuracy of ±0.05 °C.

III. Results

Gas phase spectra of the series of $Cr(CO)_5$(olefin) complexes produced by the photolysis of $Cr(CO)_6$ in the presence of these olefins have not been published before. Figure 2 gives 0.5 cm^{-1} resolution spectra for each of the complexes formed as observed immediately upon 308 nm irradiation of a mixture of $Cr(CO)_6$, CO, and olefin at 20 °C. The initial infrared spectrum of $Cr(CO)_6$ is subtracted from each spectrum.

Close examination of the strongest CO features in each of these spectra shows systematic shifts to lower wavenumber with increased substitution. Fluoroalkene complexes of $Cr(CO)_6$ and $Fe(CO)_5$ exhibit a shift to higher wavenumber.[7] Such shifts in position are often attributed to the electron donor capacity of the ligand.

Both solution and gas phase studies have established that the thermal decomposition of olefin complexes of $M(CO)_x$ ($x = 4$, 5, 6) follows a simple dissociative mechanism:[4,8,9]

$$M(CO)_5(olefin) \overset{k_1}{\rightleftharpoons} M(CO)_5 + olefin$$

$$M(CO)_5 + CO \xrightarrow{k_3} M(CO)_6 \qquad (1)$$

The rate expression for dissociative substitution is commonly reduced, by treatment of $M(CO)_5$ as a steady state intermediate, to

$$rate = k_{obs}[M(CO)_5(olefin)] \qquad (2)$$

where the observable rate constant is given by

$$k_{obs} = \frac{k_1}{((k_2/k_3)R + 1)} \qquad (3)$$

In equation 3, k_1 is the elementary rate constant for unimolecular decomposition, k_2/k_3 represents the branching ratio of olefin to CO recombination with $M(CO)_5$, and R is the ratio of [olefin] to [CO].

Over all temperatures investigated, plots of k_{obs} versus R for decomposition of the $Cr(CO)_5$(olefin) complexes reveal no deviation from eq 3 for values of R ranging from 0.01 to 5000. An example showing the composition dependence of k_{obs} for the propylene complex at 20 °C is plotted in Figure 3. In order to confirm that observed rates are not affected by heterogeneous catalysis at the stainless steel cell wall, the cell is fitted with a glass liner. Average values of k_{obs} are reproduced to within 5% uncertainty over the full range of temperatures.

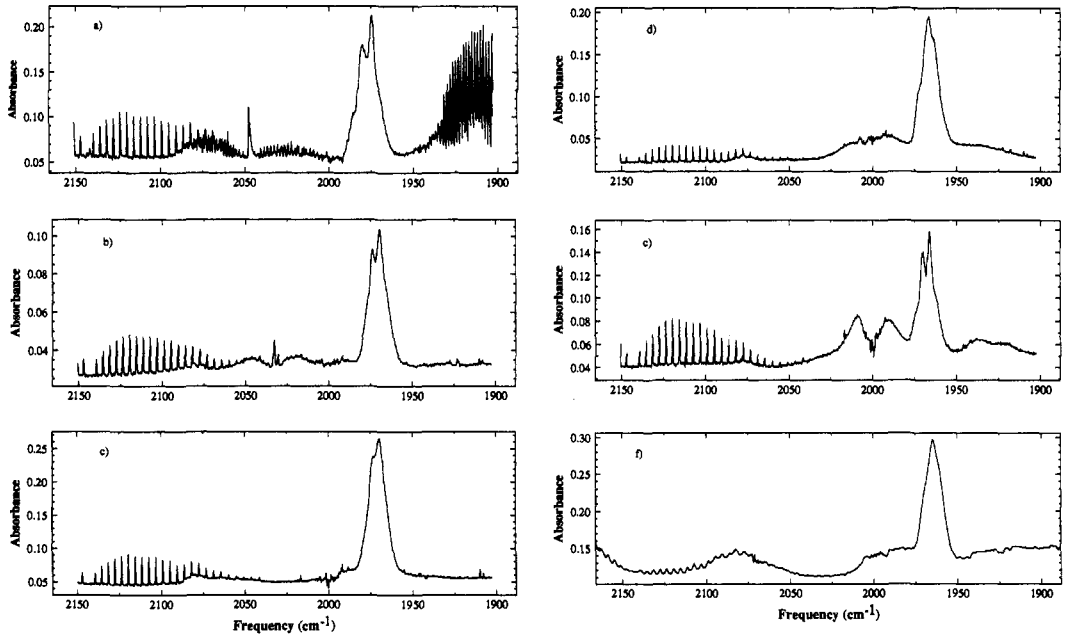

Figure 2. High-resolution infrared spectra of $Cr(CO)_5$(olefin) complexes in the CO stretching region: (a) $Cr(CO)_5(C_2H_4)$, (b) $Cr(CO)_5(C_3H_6)$, (c) $Cr(CO)_5(1\text{-}C_4H_8)$, (d) $Cr(CO)_5(cis\text{-}2\text{-}C_4H_8)$, (e) $Cr(CO)_5(trans\text{-}2\text{-}C_4H_8)$, (f) $Cr(CO)_5(i\text{-}C_4H_8)$.

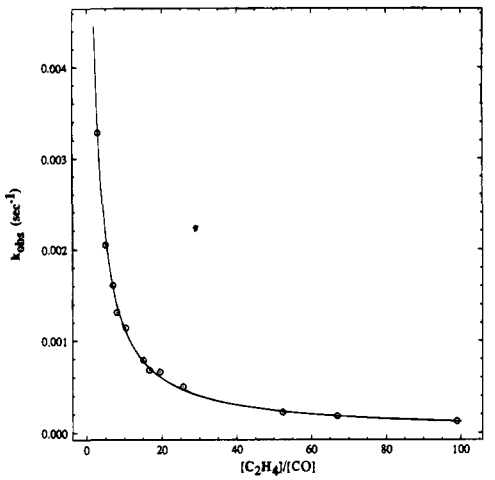

Figure 3. k_{obs} versus [olefin]/[CO] according to eq 3 at 20 °C for the propylene complex. Unique fitting for k_1 and k_2/k_3 requires high precision in k_{obs}.

Unique determination of k_1 by a nonlinear fit to eq 3 requires a high degree of precision in the k_{obs} data set. We have found that, for $M(CO)_x$ (olefin) systems in general, a very great effort in FTIR data collection can be required to obtain that precision. This is caused by a strong linear dependence in eq 3 that correlates determinations of k_1 with k_2/k_3.[4a] However, given an accurate, external measure of k_1, FTIR relaxation rates can provide an estimate of k_2/k_3 as can be seen from the slope term in the linearized version of eq 3:

$$\frac{1}{k_{obs}} = \frac{1}{k_1} + \frac{k_2}{k_1 k_3} R \qquad (4)$$

Direct measurement of k_1 is possible if the reaction can be saturated in CO. Under saturation conditions [CO] ≫ [olefin], such that $(k_2/k_3)R \ll 1$, and eq 3 reduces to

$$k_{obs} = k_1 \qquad (5)$$

Under these conditions, using the faster temporal response of the TRIR apparatus, k_1 can be determined directly. In combination with the FTIR data, an improved estimate of k_2/k_3 is then possible, through eq 3 or 4.

Table 1 lists the measured values of k_{obs} reflecting both composition and temperature dependence for the six olefin complexes. Lower-temperature measurements especially can be seen to closely approach saturation in CO. In such cases eq 5 is obeyed to within the noise of the measurement. Plots of $1/k_{obs}$ versus [olefin]/[CO] are shown in Figure 4. Figure 5 presents a detailed plot showing the approach to saturation determined by TRIR measurements on complexes of propene, *cis*-2-butene, and *trans*-2-butene. Overall, the plots reflect the trend mentioned above in which rates increase with increasing alkyl substitution. Details of this behavior are determined by the values of the constituent elementary rate constants in eq 3.

Values of k_1 obtained by direct measurement or by fits of the TRIR data to eq 4 are presented in Table 2. k_1 results reported here for the C_2H_4 complex are roughly twice those we reported previously.[4a] Despite the large k_{obs} data set used in earlier experiments (FTIR only), two-parameter fits to eq 3 or 4 yield less accuracy in determining k_1 (and k_2/k_3).

Taking our results for k_1, we are able to execute one-parameter fits to the FTIR and TRIR data. Values of k_2/k_3 obtained in this fashion are listed in Table 3. The uncertainty in k_2/k_3 has contributions from the error in both the TRIR measurement, which determines k_1, and the FTIR measurement, which gives k_2/k_1k_3. However, some important trends emerge. Olefin complex formation is favored over CO recombination in every case, and a slight increase in the rate of formation of the olefin complex appears to accompany increased alkyl substitution. This trend is also observed for recombination in the $W(CO)_5$(alkane)[10] and CpRhCO(alkane) series.[11]

$Cr(CO)_5(C_2H_4)$, $Cr(CO)_5(C_3H_6)$, and $Cr(CO)_5$(1-C_4H_8). Comparison of the data in Table 1 shows that, in general, k_1 closely parallels k_{obs} for each olefin complex. The observed decomposition rate constant, k_{obs}, with [olefin]/[CO] = 0.5 and at T = 70 °C, for the ethylene complex is roughly 4.1 times slower than that for the decomposition of the propylene complex under the same conditions. The elementary rate for decomposition, k_1, is 3.7 times slower. k_2/k_3 is nearly the same for these two ligands, and any temperature dependence in this ratio is small enough to be obscured by the uncertainty of the measurement. On this basis, any difference in the activation energies for olefin versus CO recombination can be estimated to be less than 1 kcal/mol.

The 1-butene complex decomposes with an elementary rate constant, k_1, which at room temperature is approximately 1.7 times greater than that of the propene complex. The observed rate for decomposition of the two complexes, however, is essentially indistinguishable. This effect is caused by k_2/k_3 which is slightly greater for $Cr(CO)_5$(1-butene). Table 2 lists the increase in k_1 as $Cr(CO)_5(C_2H_4) < Cr(CO)_5(C_3H_6) < Cr(CO)_5$(1-$C_4H_8$). This order matches trends seen for NiL_3(olefin), $CpMn(CO)_2$(olefin), and Ag^+(olefin) decomposition reactions.[8,9,12]

$Cr(CO)_5$(*cis*-C_4H_8), $Cr(CO)_5$(*trans*-C_4H_8), and $Cr(CO)_5$(*i*-C_4H_8). k_{obs} increases again by roughly a factor of 3−4 between the *cis*- and *trans*-2-butene complexes. This result conforms with similar observations in the solution phase literature of metal−olefin *cis*/*trans* complexes.[9] The isobutene complex decomposes with a k_{obs} nearly the same as the *trans* complex. Thus, among the secondary butenes, the *cis* complex stands out as distinctively slow. One source of the difference in the observed rate is the smaller value of k_2/k_3 for the formation of the *trans* complex which manifests itself as an increase in k_{obs}. The *cis*-olefin reacts faster with unsaturated $M(CO)_5$ than the *trans*-olefin. This result is consistent with a large body of literature concerning the enhanced reactivity of *cis*-2-butene relative to the *trans* isomer.[13] Inspection of Table 1 shows, however, that most of the difference in k_{obs} between the 2-butenes, as is the case for all of the substituted olefin chromium carbonyl complexes, lies in k_1 itself.

Activation Parameters. The systematic variation in k_1 with leaving olefin establishes that the fundamental stability of carbonyl chromium olefin complexes declines rapidly with

(6) McNamara, B. Ph. D. Thesis, Purdue University, West Lafayette, IN, 1995.

(7) (a) Reference 6, Chapter V. (b) Wells, J. R.; House, P. G.; Weitz, E. *J. Phys. Chem.* **1994**, *98*, 8343.

(8) (a) Tolman, C. A. *J. Am. Chem. Soc.* **1974**, *96*, 2780. (b) Tolman, C. A. *J. Am. Chem. Soc.* **1974**, *96*, 2740.

(9) (a) Wrighton, M.; Hammond, G. S.; Gray, H. B. *J. Am. Chem. Soc.* **1971**, *93*, 6048. (b) Wrighton, M.; Hammond, G. S.; Gray, H. B. *J. Organomet. Chem.* **1970**, *70*, 283.

(10) (a) Ishikawa, Y.; Hackett, P. A.; Rayner, D. M. *J. Phys. Chem.* **1989**, *93*, 652. (b) Ishikawa, Y.; Hackett, P. A.; Rayner, D. M. *Chem. Phys. Letts.* **1988**, *145*, 5, 4229. (c) Ishikawa, Y.; Brown, C., E.; Hackett, P. A.; Rayner, D. M. *J. Am. Chem. Soc.* **1990**, *112*, 2530. (d) Ishikawa, Y.; Brown, C., E.; Hackett, P. A.; Rayner, D. M. *Chem. Phys. Letts.* **1988**, *150*, 6, 506.

(11) Wasserman, E. P.; Moore, C. B.; Bergman, R. G. *Science* **1992**, *255*, 315 and references therein.

(12) (a) Muhs, M. A.; Weiss, F. T. *J. Am. Chem. Soc.* **1962**, *84*, 4697. (b) Cvetanovic, R. J.; Duncan, F. J.; Falconer, W. E.; Irwin, R. S. *J. Am. Chem. Soc.* **1965**, *87*, 1827. (c) Quinn, H. W.; McIntyre, J. S.; Peterson, D. **1965**, *Can. J. Chem. 43*, 2896.

(13) See for example: Roberts, J. D.; Caserio, M. C. *Basic Principles of Oranic Chemistry;* Benjamin: New York, 1965.

Table 1

(a) Phenomenological Rate Constants, k_{obs}, Observed as a Function of $[C_2H_4]/[CO]$ in the CO-for-C_2H_4 Dissociative Substitution Reaction of $Cr(CO)_5(C_2H_4)$

	$k_{obx}(s^{-1})$								
ratio	20 °C	30 °C	40 °C	50 °C	60 °C	70 °C	80 °C	90 °C	100 °C
0.050		0.159 ± 0.007	0.559 ± 0.03	1.95 ± 0.008	6.00 ± 0.73	17.5 ± 2.9	46.2 ± 5.4	119 ± 12.3	298.6 ± 13.6
0.100		0.156 ± 0.005	0.544 ± 0.01	1.86 ± 0.41	5.55 ± 0.63	16.2 ± 2.4	43.1 ± 4.3	109 ± 5.6	264 ± 11.1
0.200		0.140 ± 0.006	0.503 ± 0.03	1.67 ± 0.2	4.99 ± 0.11	14.6 ± 0.36	39.3 ± 0.96	98.5 ± 7.8	242 ± 21
0.300		0.120 ± 0.009	0.408 ± 0.06	1.35 ± 0.16	4.05 ± 0.11	11.8 ± 0.27	30.8 ± 0.44	78.7 ± 3.5	192 ± 9.1
0.400		0.108 ± 0.009	0.368 ± 0.02	1.22 ± 0.015	3.75 ± 0.18	10.7 ± 0.12	28.5 ± 1.4	73.6 ± 2.7	179 ± 13
0.500		0.053 ± 0.002	0.332 ± 0.008	1.13 ± 0.03	3.38 ± 0.19	9.59 ± 0.2	26.3 ± 0.28	68.1 ± 3.1	168 ± 11
3.00	0.00327 ± 0.00007	0.01268 ± 0.00010	0.0498 ± 0.0008	0.1867 ± 0.0085	0.5902 ± 0.0267				
5.00	0.00207 ± 0.00002	0.00850 ± 0.00033	0.030 ± 0.005	0.1267 ± 0.0067	0.394 ± 0.047				
6.9	0.00162 ± 0.00010	0.00633 ± 0.00017	0.0233 ± 0.0025	0.09017 ± 0.00083	0.297 ± 0.055				
8.00	0.00133 ± 0.00005	0.00567 ± 0.00017	0.0203 ± 0.0005	0.0817 ± 0.0033	0.2667 ± 0.0017				
10.4	0.00113 ± 0.00008	0.00417 ± 0.00017	0.0170 ± 0.0005	0.06333 ± 0.00083	0.213 ± 0.016				
15.1	0.00078 ± 0.00007	0.00327 ± 0.00012	0.0121 ± 0.0005	0.0450 ± 0.0017	0.1467 ± 0.0050				
16.6	0.00068 ± 0.00005	0.00283 ± 0.00017	0.0112 ± 0.0002	0.0377 ± 0.0017	0.135 ± 0.008				
19.5	0.00065 ± 0.00012	0.00250 ± 0.00017	0.01033 ± 0.00013	0.0350 ± 0.0013	0.115 ± 0.005				
25.6	0.00050 ± 0.00010	0.00197 ± 0.00007	0.00733 ± 0.00017	0.0250 ± 0.0033	0.085 ± 0.003				
52.3	0.00022 ± 0.00003	0.00102 ± 0.00002	0.00367 ± 0.00005	0.0140 ± 0.0005	0.046 ± 0.010				
66.9	0.00018 ± 0.00002	0.00080 ± 0.00005	0.00273 ± 0.00010	0.0107 ± 0.0005	0.0350 ± 0.0067				
99.0	0.00013 ± 0.00000	0.00053± 0.00002	0.00192 ± 0.00002	0.0073 ± 0.0005	0.02317 ± 0.00083				

(b) Phenomenological Rate Constants, k_{obs}, Observed as a Function of $[C_3H_6]/[CO]$ in the CO-for-C_3H_4 Dissociative Substitution Reaction of $Cr(CO)_5(C_3H_6)$

	$k_{obs}\,(s^{-1})$								
ratio	20 °C	30 °C	40 °C	50 °C	60 °C	70 °C	80 °C	90 °C	100 °C
0.10			2.35 ± 0.53	7.76 ± 0.36	23.9 ± 1.8	68.7 ± 14	188 ± 23	496 ± 41	1207 ± 220
0.15			1.90 ± 0.49	6.44 ± 0.35	19.33 ± 1.5	56.8 ± 12	155 ± 18	395 ± 30	972 ± 85
0.20			1.73 ± 0.05	5.72 ± 0.095	17.60 ± 1.04	50.5 ± 1.3	139 ± 8	363 ± 16	894 ± 33
0.30			1.86 ± 0.07	5.58 ± 0.24	16.8 ± 0.8	48.8 ± 1.7	131 ± 4.9	334 ± 6.8	821 ± 11
0.40			1.54 ± 0.1	4.97 ± 0.2	14.9 ± 0.3	46.0 ± 2.5	120 ± 7	311 ± 12	755 ± 24
0.500			1.31 ± 0.08	4.34 ± 0.05	13.3 ± 0.22	39.1 ± 1.3	103 ± 2.3	263 ± 9.3	634 ± 18.5
3.00	0.012 ± 0.002	0.051 ± 0.002	0.203 ± 0.04	0.768 ± 0.03	2.53 ± 0.08				
5.00	0.0083 ± 0.0002	0.034 ± 0.001	0.125 ± 0.003	0.423 ± 0.008	1.33 ± 0.2				
8.0	0.0061 ± 0.0003	0.022 ± 0.002	0.083 ± 0.003	0.315 ± 0.02	0.98 ± 0.03				
10.4	0.0044 ± 0.0002	0.0167 ± 0.0005	0.071 ± 0.003	0.262 ± 0.03	0.86 ± 0.03				
15.0	0.0032 ± 0.0002	0.012 ± 0.001	0.046 ± 0.002	0.172 ± 0.009	0.57 ± 0.03				
19.5	0.0024 ± 0.0002	0.0090 ± 0.0003	0.040 ± 0.002	0.152 ± 0.01	0.51 ± 0.02				
25.7	0.0021 ± 0.0002	0.0078 ± 0.0002	0.028 ± 0.002	0.089 ± 0.002	0.27 ± 0.02				
52.3	0.0010 ± 0.0001	0.0039 ± 0.0002	0.015 ± 0.002	0.058 ± 0.002	0.18 ± 0.01				

(c) Phenomenological Rate Constants, k_{obs}, Observed as a Function of $[1\text{-}C_4H_8]/[CO]$ in the CO-for-1-C_4H_8 Dissociative Substitution Reaction of $Cr(CO)_5(1\text{-}C_4H_8)$

	$k_{obs}\,(s^{-1})$								
ratio	20 °C	30 °C	40 °C	50 °C	60 °C	70 °C	80 °C	90 °C	100 °C
0.025		1.42 ± 0.3	5.03 ± 0.018	16.9 ± 2.1	52.2 ± 3	152 ± 24	398 ± 21	1042 ± 99	2659 ± 219
0.050		1.50 ± 0.38	4.8 ± 1.3	17.5 ± 2.7	52.4 ± 3.4	153 ± 32.5	403 ± 34	1027 ± 217	2591 ± 231
0.10		1.19 ± 0.45	4.11 ± 0.43	14.2 ± 1.9	43.2 ± 3.4	132 ± 20.1	287 ± 26	846 ± 109	2186 ± 221
0.20		0.994 ± 0.1	3.42 ± 0.3	11.8 ± 0.7	35.8 ± 2.9	102 ± 16	270 ± 9.7	682 ± 30	1830 ± 213
0.40		0.74 ± 0.02	2.69 ± 0.3	8.87 ± 0.11	27.1 ± 3.4	83.1 ± 7.1	216 ± 11	551 ± 23	1370 ± 172
0.50		0.66 ± 0.03	2.43 ± 0.21	7.95 ± 0.23	27.3 ± 2.6	77.1 ± 9	174 ± 17	434 ± 28	1352 ± 118
5.1	0.072 ± 0.011	0.030 ± 0.002	0.15 ± 0.02	0.51 ± 0.04	1.7 ± 0.2	5.8 ± 0.5			
10.4	0.0038 ± 0.0006	0.018 ± 0.003	0.068 ± 0.02	0.288 ± 0.04	0.95 ± 0.05	3.1 ± 0.4			
15.4	0.0028 ± 0.0004	0.012 ± 0.004	0.049 ± 0.002	0.20 ± 0.1	0.65 ± 0.03	2.1 ± 0.3			
25.7	0.0016 ± 0.0004	0.0070 ± 0.0005	0.025 ± 0.006	0.098 ± 0.006	0.31 ± 0.04	0.93 ± 0.05			
52.3	0.0011 ± 0.0005	0.0037 ± 0.0004	0.016 ± 0.002	0.064 ± 0.005	0.17 ± 0.04	0.542 ± 0.07			
99.0		0.0023 ± 0.0007	0.0073 ± 0.0003	0.028 ± 0.004	0.082 ± 0.002	0.23 ± 0.05			

(d) Phenomenological Rate Constants, k_{obs}, Observed as a Function of $[cis\text{-}2\text{-}C_4H_8]/[CO]$ in the CO-for-1-*cis*-2-C_4H_8 Dissociative Substitution Reaction of $Cr(CO)_5(cis\text{-}2\text{-}C_4H_8)$

	$k_{obs}\,(s^{-1})$							
ratio	20 °C	30 °C	40 °C	50 °C	60 °C	70 °C	80 °C	90 °C
0.05		1.3 ± 0.38	4.23 ± 1.3	16.1 ± 2.7	52.4 ± 3.4	154 ± 32	441 ± 35	1206 ± 217
0.08		1.19 ± 0.43	4.10 ± 0.46	14.9 ± 1.2	47.1 ± 4.1	138 ± 18.0	407 ± 46	1072 ± 82
0.10		1.3 ± 0.44	4.7 ± 0.43	15.2 ± 1.9	40.2 ± 3.4	134 ± 20.1	345 ± 26.5	943 ± 120
0.20		0.83 ± 0.29	2.82 ± 0.34	10.6 ± 0.73	35.1 ± 2.9	105 ± 23	284 ± 9.7	745 ± 92
0.30		1.00 ± 0.25	2.44 ± 0.31	8.8 ± 0.76	29.0 ± 1.9	86.6 ± 5.9	249 ± 22	637 ± 22
10.4	0.35 ± 0.04	0.26 ± 0.01	0.16 ± 0.03	0.017 ± 0.02				
29.4	0.026 ± 0.05	0.011 ± 0.005	0.045 ± 0.003	0.18 ± 0.02				
52.3	0.0016 ± 0.0003	0.0067 ± 0.0006	0.037 ± 0.002	0.19 ± 0.02				
71.3	0.0017 ± 0.0002	0.0051 ± 0.0005	0.019 ± 0.005	0.073 ± 0.002				
99.0	0.0097 ± 0.0002	0.0035 ± 0.0006	0.015 ± 0.002	0.049 ± 0.002				

Table 1 (Continued)

(e) Phenomenological Rate Constants, k_{obs}, Observed as a Function of [*trans*-2-C_4H_8]/[CO] in the CO-for-1-*trans*-2-C_4H_8 Dissociative Substitution Reaction of $Cr(CO)_5$(*trans*-2-C_4H_8)

	k_{obs} (s^{-1})						
ratio	30 °C	40 °C	50 °C	60 °C	70 °C	80 °C	90 °C
0.05	6.06 ± 0.33	19.2 ± 1.7	69.9 ± 11.9	219 ± 39	658 ± 25	1739 ± 270	4608 ± 609
0.07	4.92 ± 0.41	18.1 ± 2.8	64.9 ± 5.1	204 ± 21	588 ± 19	1623 ± 170	4516 ± 300
0.10	4.56 ± 0.5	17.0 ± 1.2	60.4 ± 7.2	190 ± 15	548 ± 17	1473 ± 74	3924 ± 164
0.20	3.78 ± 0.32	14.0 ± 3.1	46.5 ± 7.3	154 ± 11	469 ± 22	1187 ± 91	3206 ± 220
0.30	3.18 ± 0.35	11.3 ± 2.1	39.1 ±3.1	126 ± 18	386 ± 27	976 ± 52	2686 ± 251
0.40	2.79 ± 0.28	10.5 ± 2.4	33.9 ± 2.5	112 ± 6.1	323 ± 32	826 ± 78	2399 ± 129
10.4	0.17 ± 0.02	0.66 ± 0.06	2.4 ± 0.3	8.1 ± 0.5	24.5 ± 0.7	71.1 ± 2.1	198 ± 11
52.3	0.04 ± 0.005	0.15 ± 0.03	0.53 ± 0.02	1.67 ± 0.18	5.5 ± 0.2	15.3 ± 0.9	42.7 ± 1.7
73.3	0.03 ± 0.007	0.09 ± 0.007	0.33 ± 0.02	1.09 ± 0.14	3.4 ± 0.2	9.6 ± 0.5	26.7 ±2.03
99.0	0.02 ± 0.003	0.07 ± 0.003	0.25 ± 0.02	0.81 ± 0.03	2.6 ± 0.3	7.7 ± 0.2	20.7 ± 1.9
263	0.007 ± 0.0004	0.02 ± 0.006	0.09 ± 0.005	0.30 ± 0.03	0.96 ± 0.02	2.9 ± 0.4	7.76 ± 0.3

(f) Phenomenological Rate Constants, k_{obs}, Observed as a Function of [*iso*-C_4H_8]/[CO] in the CO-for-1-*iso*-C_4H_8 Dissociative Substitution Reaction of $Cr(CO)_5$(*iso*-C_4H_8)

	k_{obs} (s^{-1})							
ratio	30 °C	40 °C	50 °C	60 °C	70 °C	80 °C	90 °C	100 °C
0.10	5.19 ± 0.09	18.1 ± 0.61	60.4 ± 2.2	187 ± 10.8	549 ± 33	1469 ± 164	3805 ± 238	9441 ± 715
0.15	4.57 ± 0.23	17.0 ± 0.59	57.1 ± 2.4	175 ± 7.7	509 ± 32.2	1385 ± 54	3626 ± 155	8857 ± 290
0.20	4.2 ± 0.36	15.4 ± 0.4	52.8 ± 0.9	160.5 ± 9.5	469 ± 47	1250 ± 40	3278 ± 136	7874 ± 218
0.33	3.61 ± 0.14	12.9 ± 0.16	43.1 ± 0.53	131 ± 40	454 ± 16	1035 ± 36	2665 ± 47	6536 ± 320
0.41	3.3 ± 0.08	12.4 ± 0.1	39.3 ± 0.6	115 ± 2.7	346 ± 5.9	936 ± 28	2447 ± 66	6061 ± 200

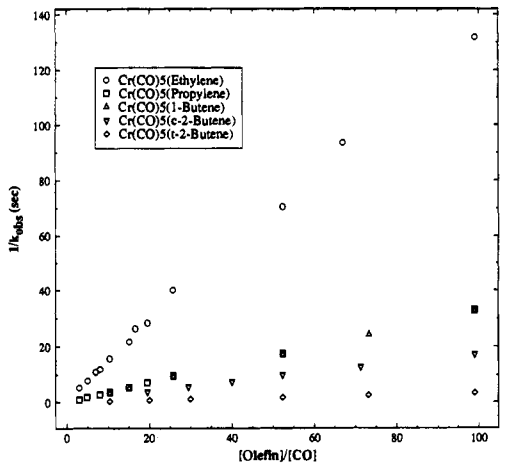

Figure 4. $1/k_{obs}$ versus [olefin]/[CO] for each ligand at 50 °C. The ethylene decay is about a factor of 40 slower than that of the *trans*-2-butene. The propylene and 1-butene rates are nearly indistinguishable. The rate of decomposition for the *trans*-butene complex is about 3.5 times greater than that for the *cis* complex. The observed rate constant for the isobutene complex (not shown) is indistinguishable from that of the *trans* complex.

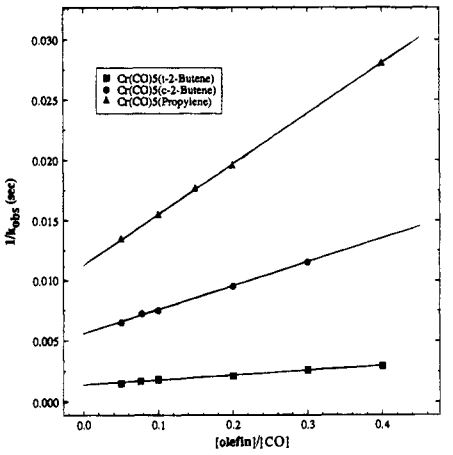

Figure 5. A detailed plot of the $1/k_{obs}$ versus [olefin]/[CO] data at 50 °C showing the approach to saturation for ligands propylene, *cis*-2-butene, and *trans*-2-butene.

Table 2. Elementary Unimolecular Rate Constants, k_1, Estimated from k_{obs} near Saturation[a]

temp	k_1 (s^{-1})					
(°C)	C_2H_4	C_3H_6	1-C_4H_8	*cis*-2-C_4H_8	*trans*-2-C_4H_8	*i*-C_4H_8
30	0.171		1.51	1.6	6.4	6.43
40	0.641	2.6	5.18	5.2	22.2	22.8
50	2.19	8.6	17.7	19.7	81.8	81.0
60	6.67	26.2	54.1	61.9	254	236
70	19.7	74.1	165	193	736	716
80	50.5	209	427	524	2061	1854
90	129.9	552	1115	1388	5319	4858
100	320.5	1339	2750			11629

[a] The uncertainty is 10−20%.

increasing substitution, exhibiting elementary decay rates in the order ethylene < propylene < 1-butene < *cis*-2-butene < *trans*-2-butene ≈ isobutene.

The data further establish, within k_1, the source of this instability. From its temperature dependence, we can resolve k_1 into its Arrhenius components, A and E_a, and then ask to what extent the acceleration in decay rate with increasing substitution affects (electronically or sterically) the metal−ligand bond energy. The answer is perhaps surprising: Arrhenius plots of $\ln(k_1)$ versus $1/T$ shown for all six olefins in Figure 6 are virtually parallel. The source of the dissociative rate increase due to alkyl substitution most decidedly does not lie in differences in the activation energy requirements for elementary metal−ligand bond cleavage. *For rate constants that range almost 2 orders of magnitude, temperature coefficients are nearly the same.*

Energies of activation and preexponential factors are listed in Table 4. On close examination, it can be seen that the measured activation energy is slightly higher for the 2-butene complexes, but this effect is just outside the uncertainty of the measurement. Such small differences in activation energy cannot account for the range observed in the elementary decay rate, which the data show is instead overwhelmingly due to variations in the preexponential (A) factor.

IV. Discussion

We have systematically measured the reaction rates for dissociative substitution in $Cr(CO)_5$(olefin) complexes for six

Table 3. Values of k_2/k_3 for Bimolecular Recombination Reactions of $Cr(CO)_5$ with Olefin Versus CO[a]

temp (°C)	k_2/k_3					
	C_2H_4	C_3H_6	1-C_4H_8	*cis*-2-C_4H_8	*trans*-2-C_4H_8	*i*-C_4H_8
30	1.8		2.6	4.4	3.3	2.3
40	2.0	1.8	2.5	4.2	2.9	2.1
50	1.9	1.9	2.4	3.8	3.5	2.4
60	1.9	1.9	2.5	3.9	3.3	2.5
70	1.9	1.8	2.5	4.2	3.0	2.6
80	2.1	2.0	2.8	4.0	3.7	2.5
90	1.9	2.1	3.1	4.1	3.1	2.6
100	1.9	2.0	2.5			2.4

[a] The uncertainty in k_2/k_3 ranges from 30 to 50%, but the trend to higher values with increasing ligand size is reproducible.

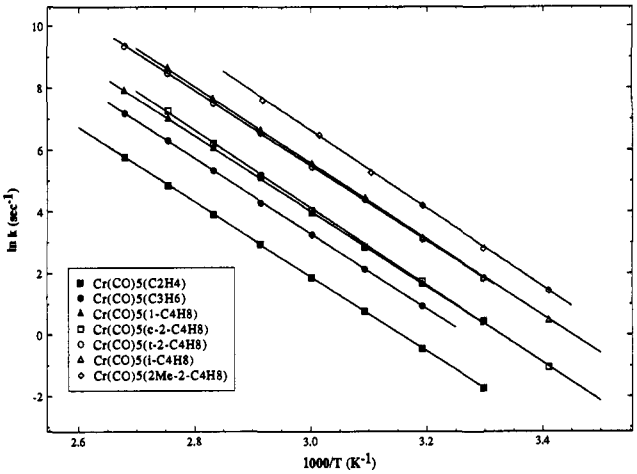

Figure 6. Arrhenius plots of $\ln(k_1)$ versus $1/T$ for all ligands. Note from the parallel straight lines that thermal activation energies are virtually identical for the entire set of ligands. Recent new data for 2-methyl-2-butene are included for comparison. Intercept differences reflect A factors that increase uniformly with increasing ligand complexity.

Table 4. Arrhenius Parameters for Elementary Unimolecular Decomposition Determined Experimentally for Each Complex from Fits of $\ln(k_1)$ versus $1/T$

complex	E_a (kcal/mol)	A (s^{-1})
$Cr(CO)_5(C_2H_4)$	24.0 ± 0.3	$(4 \pm 0.9) \times 10^{16}$
$Cr(CO)_5(C_3H_6)$	24.2 ± 0.3	$(2 \pm 0.7) \times 10^{17}$
$Cr((CO)_5(1\text{-}C_4H_8)$	24.2 ± 0.3	$(4 \pm 1.3) \times 10^{17}$
$Cr(CO)_5$(*cis*-2-C_4H_8)	24.8 ± 0.3	$(1 \pm 0.5) \times 10^{18}$
$Cr(CO)5$(*trans*-2-C_4H_8)	24.6 ± 0.3	$(4 \pm 1.5) \times 10^{18}$
$Cr(CO)_5$(*i*-C_4H_8)	24.1 ± 0.3	$(2 \pm 0.6) \times 10^{18}$
$Cr(CO)_5$(2-Me-2-C_4H_8)	24.5 ± 0.4	$(6 \pm 2.7) \times 10^{18}$

olefins ranging from ethylene to isobutene. Determinations of rates of conversion from $Cr(CO)_5$(olefin) to $Cr(CO)_6$, for more than 2000 samples ranging over 5 orders of magnitude in relative concentrations of competing ligands, establish elementary rate constants for the primary step of $Cr(CO)_5$(olefin) thermal unimolecular decomposition, and relative rate constants for bimolecular recombination of $Cr(CO)_5$ with CO and each of the six olefins. The temperature dependence of these rate constants yields absolute Arrhenius parameters for elementary metal−ligand bond scission. The results are definitive and reveal distinctive trends in metal−ligand recombination rates and the factors that regulate stability with respect to metal−ligand bond scission.

Metal−Ligand Recombination Rates. A review of the gas phase rate constants for bimolecular addition of an assortment of reactants with photoprepared $W(CO)_5$ and $Cr(CO)_5$ has recently been published.[14] In the majority of the systems investigated, the incoming ligand has been a classically unreactive species. There have been no systematic studies of recombination rates for conventional ligands such as amines, phosphines, alkynes, and alkenes, in the gas phase, despite the existence of a well-defined methodology for such measurements. Bimolecular coordination reactions with coordinatively unsaturated $M(CO)_5$ occur at near gas kinetic rates. This implies a generally low activation barrier to product formation for these processes.

The magnitudes of the rates of recombination are highly uniform. Ninety percent of the rate constants measured thus far fall between 1×10^6 and 2×10^6 $Torr^{-1}$ s^{-1}. There appears to be little steric influence on recombination, as rates for smaller ligands, such as H_2, N_2, and CO, are similar to those for the alkanes.[10] Reaction probabilities based on a simple hard sphere collision estimate reproduce experimental trends within a family of ligands, but do not account for the measured differences in rates of ligand recombination for dissimilar ligands. This implies that ligand electronic effects have a role in the recombination step.

Available determinations[15] of the CO recombination rates with unsaturated $Cr(CO)_5$ range between 0.22×10^6 and 1.3×10^6 $Torr^{-1}$ s^{-1}, lending uncertainty to any absolute estimate of the rate constants for metal−olefin recombination, k_2, from our k_2/k_3 data. For the six olefins studied here, k_2 appears to be a factor of 2 or 3 larger than k_3. Methyl substitution increases the σ donor ability of the alkenes, and rate enhancement over the series from ethylene to the butenes may reflect an increasing nucleophilic character. Apart from the hydrocarbon/fluorocarbon results cited above, there are few or no recombination rate data in the gas phase literature, for ligands with systematically varying σ donor or π^* acceptor properties, to offer support for this conclusion.

Some researchers have speculated that metal η^2-alkene coordination may be preceded by σ coordination.[16] Branching ratios (k_2/k_3) listed in Table 3 imply a small increase in k_2 with ligand size. This trend has not been observed in solution for smaller alkenes, but was reported for C_6 alicyclic alkenes.[9] The same trend is noted for alkane binding with $W(CO)_5$,[10] and in Rh(CO)(alkane) complexes.[11] In this regard, comparison of bimolecular rates for alkene versus alkane addition to $M(CO)_5$ would be interesting.

Activation Parameters E_a and A. The magnitudes of the activation energies that we measure seem appropriate, as the bond energy of $Cr(CO)_5$(olefin) should lie between those of Cr−CO and Cr−alkane. The measured range of elementary rates agrees with general trends in the solution phase literature, where metal−olefin decomposition rate constants are observed to increase with increasing olefin complexity.

Remarkably, the activation energies we observe establish that this stability trend has little to do with binding energies in the complexes. Instead, we find that the persistent increase in rate with increasing alkyl substitution is driven almost entirely by the preexponential factors of the temperature-dependent elementary unimolecular rate constants.

Preexponential factors associated with loose transition states normally measure 10^{15} s^{-1} or more. For larger polyatomics this value can be orders of magnitude larger. From the perspective of transition state theory, A factors exceeding kT/h (ca. 10^{-13} s^{-1}) must arise from a positive entropy of activation,

(14) Weitz, E. *J. Phys. Chem.* **1994**, *98*, 11256.

(15) Weitz, E. *J. Phys. Chem., Rev.* **1991**.

(16) (a) Stoutland, P. O.; Bergman, R. G. *J. Am. Chem. Soc.* **1985**, *107*, 4581. (b) Stoutland, P. O.; Bergman, R. G. *J. Am. Chem. Soc.* **1988**, *110*, 5732. (c) Zhang, S.; Dobson, G. R.; Zang, V; Bajaj, H. C.; van Eldik, R. *Inorg. Chem.* **1989**, *29*, 3478. (d) Kafifi, Z. H.; Hauge, R. H.; Margrave, J. L. *J. Am. Chem. Soc.* **1985**, *107*, 7550. (e) Bell, T. W.; Haddleton, D. M.; McCawley, A.; Partridge, M. G.; Perutz, R. N.; Willner, H. *J. Am. Chem. Soc.* **1990**, *112*, 9212.

Table 5. RRKM Model Frequencies Chosen for Metal−Olefin Vibrations in the Activated Molecule That Correlate to Free Olefin Translations and External Rotations upon Dissociation

metal−ligand frequencies in the activated molecule (cm^{-1}) $Cr(CO)_5$(Olefin)	metal−ligand frequencies in the critical configuration (cm^{-1})[a]					
	$Cr(CO)_5$ (C_2H_4)	$Cr(CO)_5$ (C_3H_6)	$Cr(CO)_5$ (1-C_4H_8)	$Cr(CO)_5$ (*cis*-2-C_4H_8)	$Cr(CO)_5$ (*trans*-2-C_4H_8)	$Cr(CO)_5$ (*i*-C_4H_8)
450	108	88	76	76	76	76
430	103	84	73	73	73	73
360	86	70	61	61	61	61
350	84	69	59	59	59	59
320	77	63	54	54	54	54
400	r†	r†	r†	r†	r†	r†

[a] These frequencies are taken to be the same for all complexes, except for a factor that scales critical-configuration metal−olefin frequencies for the total mass of the pendant olefin.

reflecting a tendency toward increasing disorder in degrees of freedom orthogonal to the reaction coordinate. Positive entropies of activation are expected for simple bond scission reactions and reflect the conversion of fragment bending and torsional vibrations into incipient free translations and rotations as the fragment separation coordinate passes through the critical configuration.

In addition to these closely coupled vibrational degrees of freedom, which are common to all dissociating metal−ligand systems, the substituted olefins have low-frequency torsions and skeletal bends. These low-frequency modes are likely to be among those most affected by coordination and thus another source of difference between the coordinated olefin and the free olefin—between the coordinated complex and its transition state for metal−olefin bond scission. Repulsive effects on substituent groups in larger olefins coordinated to chromium carbonyl have been characterized theoretically by White and Brown.[3] Though not explicitly considered in that work, repulsive interactions must constrain low-frequency motion, thereby raising vibrational frequencies in the coordinated olefin. Relowering of these frequencies, then, as the system progresses from the bound complex to the transition state, introduces disorder. Adding to $\Delta S^{\ddagger}$, this addition to the state density serves to increase the *A* factor. The greater the number of low-frequency modes affected, the greater the effect and therefore the larger the enhancement of the *A* factor for thermal unimolecular decomposition.

Thus, considering the possible behavior of the low-frequency modes of the ligands alone, we can qualitatively explain the trends that we find in metal−ligand decomposition rates. It is important now to inquire whether a computational model incorporating an idea such as this can account quantitatively for the temperature dependence observed in the elementary decay constants across the entire series of ligands. To develop a more convincing foundation for this model, we have carried out a set of RRKM calculations.[17] The results lend support to the simple physical picture of released low-frequency motion as a statistical driving force accelerating the unimolecular decomposition of substituted olefin complexes.

A Simple RRKM Model for the Thermal Unimolecular Decomposition of Chromium Olefin Carbonyls. We suggest that low-frequency vibrations, which are stiffened in the coordinated ligand and released in the transition state, contribute significantly to the declining stability of the higher substituted olefin complexes. Our ligand set is complete to C_4, and we can test this hypothesis for self-consistency by performing a series of RRKM calculations.

Among the inputs required is a set of vibrational frequencies for the complex and the critical configuration (transition state). In addition to the frequencies, a minimal RRKM calculation requires the potential energy as a function of displacement along the reaction coordinate, and the moments of inertia of the reactant and critical configuration.

The vibrational frequencies determine the state density of the reactant molecule, and the sum of states in the critical configuration. The potential function establishes the threshold energy, and the moments of inertia determine the fraction of overall rotational energy that can contribute to the dissociation.

To isolate the issue of constrained low-frequency vibrational degrees of freedom and their effect on rates, we adopt a simple uniform model for the decomposition of all six complexes. This model incorporates a constant set of core RRKM parameters, which apply to the entire series of olefin-substituted chromium carbonyls, together with parameters specific to the size and structure of the leaving olefin which vary systematically with alkyl substitution.

Thus, we use the same reaction coordinate potential for all six metal-olefin bond scissions. Vibrational frequencies associated with the $Cr(CO)_5$ fragment, in both the complex and critical configuration, come from a reduced set of frequencies assigned to $Cr(CO)_6$, and are held constant for the entire series. Different choices for these frequencies, which have the same values in the complex and critical configuration, cause little or no change in the computed rate constant.

The six frequencies associated with the vibrational motion of the metal−olefin linkage have not yet been determined for the subject compounds by either experiment or ab initio calculations. However, reasonable estimates can be made from the infrared spectra of iron− and osmium−olefin complexes.[18-21] Frequency values so estimated are also taken to be the same for all complexes.

As dissociation proceeds, these metal−olefin modes become the incipient translational and rotational degrees of freedom of the free ligand. The loosening of these frequencies in the critical configuration constitutes the main adjustable parameter in fitting a RRKM calculation to an observed rate. We choose a frequency reduction to give agreement between calculation and experiment for ethylene. Thereafter, we hold these critical configuration frequencies constant, except for a factor that accounts for the increase in total mass of the C_3 and C_4 ligands pendant in the transition state (cf. Table 5). The mass of the leaving ligand also determines moments of inertia in the complex and critical configuration.

The remaining frequencies to be defined for each critical configuration are those of the leaving olefin. These are simply

(17) (a) Robinson, P. J.; Holbrook, K. A. *Unimolecular Reactions;* Wiley-Interscience: New York, 1972. (b) Gilbert, R. G.; Sean, S. C. *Theory of Unimolecular and Recombination Reactions;* Blackwell Scientific Publications: Oxford, 1990.

(18) Andrews, D. C.; Davidson, G. *J. Organomet. Chem.* **1972**, *35*, 161.
(19) Bigorne, M. *J. Organomet. Chem.* **1978**, *160*, 345.
(20) Miller, M. E.; Grant, E. R. *J. Am. Chem. Soc.* **1987**, *109*, 7951.
(21) Anson, C. E.; Johnson, B. F. G.; Lewis, J.; Powell, D. B.; Shepard, N.; Bhattacharya, A. K.; Bender, B. R.; Bullock, R. M.; Hember, R. T.; Norton, J. R. *J. Chem. Soc., Chem. Commun.* **1989**, 703. Anson, C. E.; Powell, D. B.; Shepard, N.; Bender, B. R.; Norton, J. R. *J. Chem. Soc., Faraday Trans.* **1994**, *90*, 1449.

Table 6. RRKM Model Frequencies (cm^{-1}) for Ligand Torsions and C−C−C Skeletal Bending Vibrations Chosen To Be Tightened to Values (ν^*) in the Bound Complex and To Have Free Ligand Values ($\nu^\dagger$) in the Critical Configuration

$Cr(CO)_5(C_2H_4)$		$Cr(CO)_5(C_3H_6)$		$Cr(CO)_5(1\text{-}C_4H_8)$		$Cr(CO)_5(cis\text{-}2\text{-}C_4H_8)$		$Cr(CO)_5(trans\text{-}2\text{-}C_4H_8)$		$Cr(CO)_5(i\text{-}C_4H_8)$	
ν^*	$\nu^\dagger$	ν^*	$\nu^\dagger$	ν^*	$\nu^\dagger$	ν^*	$\nu^\dagger$	ν^*	$\nu^\dagger$	ν^*	$\nu^\dagger$
		854	427	594	297	780	390	588	294	832	416
		312	156	252	126	624	312	964	241	1058	382
						366	183	410	205	406	203
						258	129	532	133	772	193

taken from well-established vibrational assignments of the free olefins.[22] The same frequency sets are used to describe the internal vibrations of fully coordinated olefins, except for a few low-frequency torsion and skeletal bending modes, which are systematically tightened using the following rationale.

We assign the ligands to one of three groups, according to the degree to which coordination is assumed to affect low-frequency vibrational motion. The first group contains only ethene. For calculations involving this ligand, no frequencies are tightened: Chromium carbonyl bound ethylene is assumed to have the same vibrational frequencies as free ethylene and ethylene in the critical configuration for unimolecular decomposition.

The second group includes propene, 1-butene, and *cis*-2-butene. For each of these ligands, constraints on low-frequency vibration are balanced against overall CO−alkyl substituent repulsion. For propene and 1-butene, we assume that the two lowest frequencies, which are assigned to methyl torsion and C−C−C skeletal bend, are doubled on coordination. In similar fashion for coordinated *cis*-2-butene, we simply double two methyl torsion and two skeletal bending frequencies.

The third group contains *trans*-2-butene and isobutene. Here, the repulsion of one alkyl substituent necessarily rocks the other into closer proximity and presumably stronger interaction with neighboring CO ligands. We account for this arbitrarily by simply quadrupling one torsion−bend pair while doubling the other. The free olefin frequencies affected by the model just described and their assumed values upon coordination are summarized for all six complexes in Table 6.

Gas phase elementary thermal unimolecular decomposition rates in general are rather insensitive to molecular size. Thus, when we run RRKM calculations in which we change frequencies only for the five metal−ligand modes directly involved in the bond scission (by the same amount), we obtain nearly the same Arrhenius parameters for all six reactions ($\log A = 16.6$ s^{-1}, $E_a = 23.8$ kcal mol^{-1}). Even when we scale the critical-configuration metal−olefin frequencies to allow for increasing leaving ligand mass, $\log A$ ranges only from 16.6 to 17.1 s^{-1} (cf. Table 7). However, when we apply the simple model described above to account for hindered low-frequency vibrations, we obtain unimolecular rate constants that increase with substitution, in quantitative accord with experiment. Table 7 compares experimental Arrhenius parameters with theoretical ones derived from this simple uniform RRKM model for elementary metalloolefin decomposition.

Structural information, including frequencies and potential energy functions, is simply not available for organometallic complexes and their critical configurations, at a level of accuracy that would permit unadjusted RRKM calculations of elementary unimolecular decomposition rate constants. Nevertheless, the ready correspondence between experiment and theory for such a simple model as the one just presented suggests that the underlying physical picture offers some relevant insight on the factors that affect stability as a function of ligand substituents. The issues encountered here, relating to the recognition of a substrate by a reaction center, have importance well beyond organometallic kinetics, and the present results underline ways in which factors other than energetic ones can provide the key basis for discrimination.

(22) See for example: Chhiba, M.; Vergoten, G. *J. Mol. Struct.* **1994**, *326*, 35−58 references therein.

Table 7. Comparison of Experimental Arrhenius Parameters with Those Obtained from RRKM Calculations Using the Model Described in the Text[a]

	experiment		RRKM calculations		
complex	E_a (kcal/mol)	$\log A$ (s^{-1})	E_a (kcal/mol)	$\log A$ (s^{-1})	$\log A^*$ (s^{-1})
$Cr(CO)_5(C_2H_4)$	24.0 ± 0.3	16.6	23.8	16.6	16.6
$Cr(CO)_5(C_3H_6)$	24.2 ± 0.3	17.3	24.2	17.2	16.8
$Cr((CO)_5(1\text{-}C_4H_8)$	24.2 ± 0.3	17.6	24.3	17.6	17.1
$Cr(CO)_5(cis\text{-}2\text{-}C_4H_8)$	24.8 ± 0.3	18.0	24.6	18.0	17.1
$Cr(CO)_5(trans\text{-}2\text{-}C_4H_8)$	24.6 ± 0.3	18.6	25.0	18.6	16.3
$Cr(CO)_5(i\text{-}C_4H_8)$	24.1 ± 0.3	18.3	24.9	18.3	17.1

[a] The column labeled $\log A^*$ gives preexponentials obtained by running all calculations, as for ethylene, without tightening torsions or C−C−C bends.

V. Conclusions

Using time-resolved infrared absorption, we have obtained elementary rates of unimolecular decomposition in the gas phase for the chromium carbonyl complexes of ethylene, propylene, 1-butene, *cis*-2-butene, *trans*-2-butene, and isobutene. Rates are observed that fit a trend of declining stability with increasing alkyl substitution. Arrhenius parameters, derived from the temperature dependence of the elementary unimolecular decay rate, establish the fundamental basis of this stability trend. Surprisingly, it lies not in decreasing bond strengths—activation energies are essentially constant for the series—but rather in a substantial increase in the A factor for larger olefin loss. This effect is explained in terms of sterically constrained torsional and C−C−C skeletal bending vibrations that are released as the molecule dissociates, adding to the statistical driving force favoring decomposition. Elementary RRKM unimolecular rate theory calculations confirm this suggestion with a uniform model for hindered low-frequency vibrations that quantitatively reproduces the observed rates.

Acknowledgment. We gratefully acknowledge support for this work from the U.S. Department of Energy under Grant No. DE-FG02-93ER14401 and the National Science Foundation under Grant No. CHE-93-07131.

JA9524199